Development of Visible Light Driven Photocatalyst for the Cost Effective Synthesis of High Value Rhodamine 110 from Rhodamine B

Dissertation submitted to
Visvesvaraya National Institute of Technology, Nagpur
In partial fulfilment of the requirements for the award of the degree

Master of Science

In

Chemistry

by

Himanshu (MS23CHM014)

under the guidance of

Dr. Atul V. Wankhade

Department of Chemistry

Visvesvaraya National Institute of Technology

Nagpur 440010 (India)

May 2025

©Visvesvaraya National Institute of Technology (VNIT) 2025

Department of Chemistry
Visvesvaraya National Institute of Technology, Nagpur

Declaration

I, Himanshu hereby declare that this dissertation titled **"Development of Visible Light Driven Photocatalyst for the Cost Effective Synthesis of High Value Rhodamine 110 from Rhodamine B"** is carried out by me in the Department of Chemistry of Visvesvaraya National Institute of Technology, Nagpur. The work is original and has not been submitted earlier whole or in part for the award of any degree/diploma at this or any other Institution / University.

Himanshu (MS23CHM014)

Date

Certificate

This is to certify that the dissertation titled **"Development of Visible Light Driven Photocatalyst for the Cost Effective Synthesis of High Value Rhodamine 110 from Rhodamine B"** is submitted by **Himanshu** in partial fulfilment of the requirements for the award of the degree of **Master of Science in Chemistry, VNIT Nagpur.** The work is comprehensive, complete and fit for final evaluation.

Dr. Atul V. Wankhade
Associate Professor
Department of Chemistry, VNIT Nagpur

Head, Department of Chemistry
VNIT, Nagpur
Date

Visvesvaraya National Institute of Technology, Nagpur

Department of Chemistry

Non-Plagiarism Certificate

Certified that M.Sc. dissertation titled **"Development of Visible Light Driven Photocatalyst for the Cost Effective Synthesis of High Value Rhodamine 110 from Rhodamine B"** submitted by **Himanshu** Enrollment No. **MS23CHM014** ID No. **30633** has been checked for plagiarism using TURNITIN software, and the overlap is found within prescribed limits. A summary of the report is given below.

Dr. Atul V. Wankhade
Associate professor
Department of Chemistry
Visvesvaraya National Institute of Technology
Nagpur (440010)

Himanshu
Enrollment no. MS23CHM014

Acknowledgment

I would like to express my sincere gratitude to my supervisor, **Dr. Atul V. Wankhade**, for his exceptional guidance, unwavering support, and invaluable mentorship throughout my journey as a M.Sc. student. I am forever indebted for his remarkable expertise, patience, and dedication in guiding me through conducting research and writing this thesis. Your astute insights, constructive feedback, and visionary guidance have been instrumental in shaping the direction of my work.

I would also like to express my gratitude to Dr. Sujit Kumar Ghosh, Head of Department, Visvesvaraya National Institute of Technology, for his invaluable support.

I would also like to express my gratitude to my Ph.D. scholars, Mr. Mohd. Amin, Mrs. Awanti S. Talmale, Ms. Sakshi Barad, Mrs. Diksha Mohod, Mr. Manoranajn Sankhua, and Mr. Adarsh Mourya, who have accompanied me on this academic journey. Your camaraderie, intellectual discussions, and collaborative efforts have enriched my experience in countless ways. Through our shared challenges and triumphs, I have not only grown as a researcher but also formed lasting friendships and a supportive network. Your diverse perspectives, stimulating debates, and willingness to lend a helping hand have been invaluable, and I am grateful for the opportunity to be part of such an inspiring community.

Furthermore, I would like to express my heartfelt gratitude to my lab mate, Ms. Saumya Meghwani, and all those who generously offered their help and support throughout this journey. At last, I sincerely dedicate my special thanks to my friends and family and staff of VNIT for their support and encouragement.

Himanshu
Id No. 30633

Abstract

Conventional methods often fall short in achieving complex organic transformations efficiently. To address this challenge, this research focuses on developing an effective photocatalyst for the selective N-deethylation of Rhodamine B (Rh-B) to Rhodamine 110 (Rh-110). Here we report the synthesis of $ZnIn_2S_4$ via the hydrothermal method, which on post modification by loading of CuS, results in the formation of $CuS/ZnIn_2S_4$ nanocomposites with varying weight percentage of CuS (2%, 4%, 6%, and 8%). These samples were thoroughly characterized using techniques such as Powder X-ray diffraction (PXRD) for crystal structure, UV-Vis diffuse reflectance spectroscopy (DRS) for band gap determination. These characterizations provided comprehensive insights into the structural and functional properties of both the base material and the synthesized nanocomposites. The deethylation of Rh-B in the presence of visible light was used to analyse the activity of $ZnIn_2S_4$, CuS, and $CuS/ZnIn_2S_4$ and it was found that only $CuS/ZnIn_2S_4$ nanocomposite was able to do so. The 4% $CuS/ZnIn_2S_4$ nanocomposite exhibited superior photocatalytic performance for the conversion of Rhodamine B (Rh-B) to Rhodamine 110 (Rh-110) in just 90 minutes. In contrast, the 8% composite showed lower conversion efficiency and a higher degree of degradation of Rh-B. Optimization studies revealed that a catalyst dosage of 10 mg of the 4% $CuS/ZnIn_2S_4$ composite is most effective in photocatalyzing this transformation. Overall, the findings highlight the photocatalytic potential of the 4% $CuS/ZnIn_2S_4$ nanocomposite, presenting a promising and efficient strategy for the selective N-deethylation of Rh-B to Rh- 110.

List of Figures

Sr. No.	Title of figure	Page No.
1.	Classification of nano-materials	3
2.	Types of synthesis of nano-materials	7
3.	Schematic equation for Rh-B to Rh-110 conversion	19
4.	P-XRD analysis of (a) $ZnIn_2S_4$, (b) CuS, (c) 2% CuS/ZIS, (d) 4% CuS/ZIS, (e) 6% CuS/ZIS, (f) 8% CuS/ZIS	25
5.	Normalised DR spectra of (a) $ZnIn_2S_4$, (b) CuS, (c) 2% CuS/ZIS, (d) 4% CuS/ZIS, (e) 6% CuS/ZIS, (f) 8% CuS/ZIS	26
6.	Tauc plot for band gap calculation of (a) $ZnIn_2S_4$, (b) CuS, (c) 2% CuS/ZIS, (d) 4% CuS/ZIS, (e) 6% CuS/ZIS, (f) 8% CuS/ZIS	27
7.	UV-Vis Spectra of the conversion of (a) 5 ppm Rh-B to Rh-110 using 10 mg 4% CuS/ZIS, (b) 7.5 ppm Rh-B to Rh-110 using 10 mg 4% CuS/ZIS, (c) 10 ppm Rh-B to Rh-110 using 10 mg 4% CuS/ZIS	31
8.	UV-Vis Spectra of conversion of 7.5 ppm Rh-B to Rh-110 using (a) 5 mg 4% CuS/ZIS, (b) 10 mg 4% CuS/ZIS, (c) 15 mg 4% CuS/ZIS	32
9.	UV-Vis Spectra of conversion of 7.5 ppm Rh-B to Rh-110 using 10 mg (a) 2% CuS/ZIS, (b) 4% CuS/ZIS, (c) 6% CuS/ZIS, (d) 8% CuS/ZIS	34
10.	Plausible Mechanism for The Conversion of Rh-B to Rh-110	35
11.	Stepwise deethylation of Rh-B	36
12.	(a) Absorption Spectra, (b) Emission Spectra, (c) Excitation Spectra of Standard Rh-110 (ST Rh-110) and photocatalytic product (Rh-110)	37

List of Contents

CHAPTER 1: INTRODUCTION 1

1.1 Nano-Materials 2

1.2 Types of Nano-Materials 3

1.3 Synthesis of Nano-Materials 6

1.4 Important Features of Nano-Materials 11

1.5 Applications of Nano-Materials 12

1.6 Nano-Materials as Photocatalyst 15

1.7 General Mechanism of Conversion of Organic Species by Photocatalyst 15

1.8 Selection of Base Material 16

1.9 Material Selected for Modification 17

1.10 Aim and Objective 18

CHAPTER 2: EXPERIMENTAL SECTION 21

2.1 Synthesis of Zinc Indium Sulfide ($ZnIn_2S_4$) 22

2.2 Synthesis of CuS/ZIS 22

CHAPTER 3: RESULT AND DISCUSSION 24

3.1 X-Ray Diffraction Analysis 25

3.1 UV DR Spectra 26

CHAPTER 4: PHOTOCATALYTIC EXPERIMENTS 29

4.1 Concentration Optimisation of Rh-B 30

4.2 Dose Optimisation 32

4.3 Comparison of Optimised Condition on composites 33

4.4 Plausible Mechanism for the Photocatalytic Transformation of Rh-B to Rh-110 35

4.5 Evidence of Rh-110 Production by Spectral Analysis 36

CHAPTER 5: CONCLUSION 38

5.1 Conclusion 39

CHAPTER 1

Introduction

1. Introduction:

The advent of nanomaterials has brought a transformative shift in material science, particularly in their role as photocatalysts. These materials have surpassed conventional boundaries in energy conversion and chemical reaction processes, paving the way toward a more sustainable future. Nanomaterials act as highly efficient catalysts, accelerating complex chemical reactions while minimizing undesired side reactions. Over the past four to five decades, challenges once deemed unsolvable are now being addressed through the unique capabilities of nanomaterials. At the heart of this advancement lies the role of photons in driving chemical transformations. Due to their nanoscale dimensions and exceptional surface properties, nanomaterials can absorb photons efficiently, enabling them to initiate and sustain chemical reactions. Unlike their bulk counterparts, nanomaterials exhibit distinct electrical and optical properties, allowing them to absorb a broader spectrum of light. This enhances their performance as photocatalysts in converting harmful pollutants into harmless substances. Today, nanomaterials can be synthesized from metal oxides, semiconductors, and carbon-based materials, each tailored for specific catalytic tasks. Their diverse properties make them highly adaptable for various environmental and energy-related applications. With their growing relevance, nanocatalysts are playing a vital role in advancing environmental sustainability.

1.1 Nano-Materials:

Materials with dimensions confined to the range of 1–100 nanometers are referred to as nanomaterials. These materials can take various forms such as tubes, dots, rods, and fibers. Due to their extremely small size and high surface-to-volume ratio, nanomaterials exhibit distinct physical and chemical properties that differ significantly from those of their bulk counterparts. Nanomaterials can be classified in several ways, and a schematic representation of their classification is provided below.

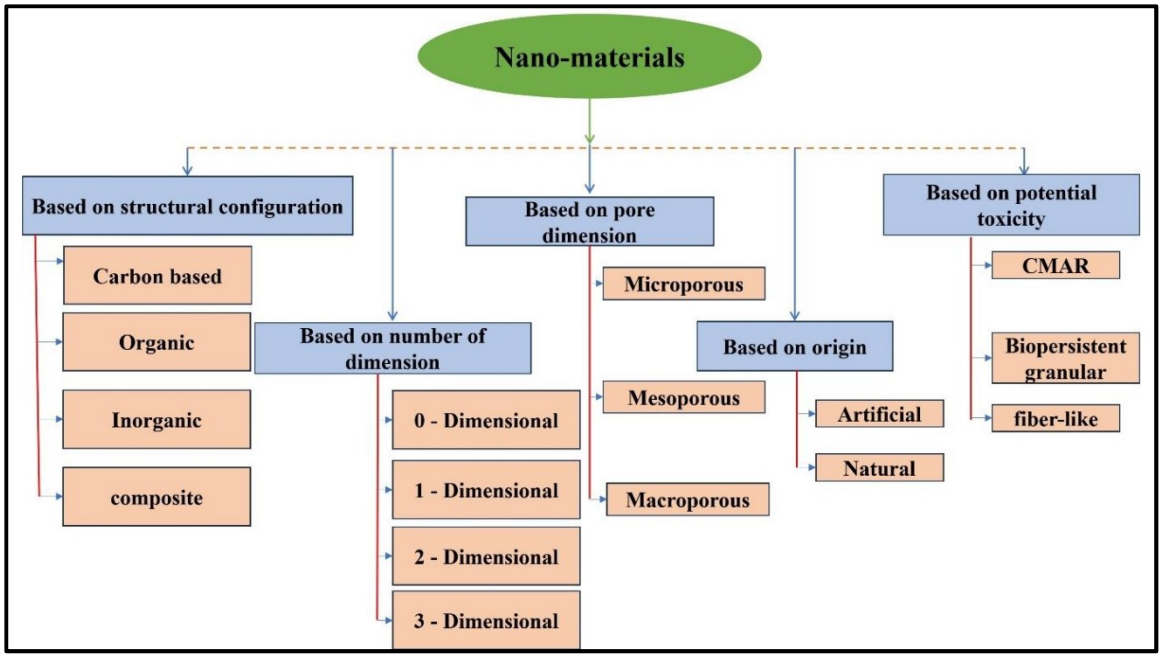

Fig.1 Classification of Nano-materials

1.2 Types of Nano-Materials:

- **Based on Structural Configuration:**

1. Carbon Based Nano-Materials:

There are so many sp^2 and sp^3 hybridized allotropes of carbon that can be made in laboratory, which are fullerenes, carbon nanotubes, graphene, Nanodiamond etc. exhibit significant properties similar to nanomaterials.

2. Organic Nano-Materials:

This type of nanomaterials is made up of organic substances which have a size lesser than 100 nm. Organic nanomaterials contain Nano films, Nano membranes, Nano scaffolds etc. The precursors of organic nanomaterials can be natural or synthetic.

3. Inorganic Nano-Materials:

These types of nanomaterials are made up of inorganic substances and the size of the materials is restricted to the nanometer range. Inorganic materials like silica, gold, silver, iron etc. are combined to form nanomaterials.

4. Composite Nano-Materials:

Composite nanomaterials are also known as nanocomposites. These are the multiphase nano size-solid materials. These types of materials form 1 dimensional or multi-dimensional matrix.

- **Based on dimensions:**

1. Zero-Dimensional Nano-Materials:

Zero-dimensional nanomaterials are the class of nanomaterials in which all dimension of material falls under the nano range, generally in between 100mn. Some examples of 0D nanomaterials are quantum dots, fullerenes, nanoclusters, nanocrystals etc.

2. One-Dimensional Nano-Materials:

In these types of nanomaterials, one of the three dimensions exceeds the nano range and has a diameter in between 100nm. Few examples of 1D nanomaterials are carbon nanotube, silver nanowire, copper nanowire, 1D polymeric nanomaterials. 1D nanomaterials have a few advantages of electron and ion transmission, light capturing ability, large surface area etc.

3. Two-Dimensional Nano-Materials:

Nanomaterials consist of two dimensions outside the nanoscale are called 2D nanomaterials. They are sheet or layer forms of materials and have one dimension in the nano range. 2D graphene, hexagonal boron nitride (h-BN), transition metal dichalcogenides (TMDCs), phosphorene etc. 2D nanomaterials can provide advanced

chemical, electrical, and optical properties. These materials have a wide range of applications in the fields of tissue engineering, drug imaging, biosensors and many more.

4. Three-Dimensional Nano-Materials:

The nanomaterials in which no dimension is limited to the nanoscale. In 3D nanomaterials macro/mesopores are interconnected that restrict aggregation. 3D nanomaterials have unique morphologies that can lead to various applications in the field of nanotechnology. Some examples of 3D nanomaterials are metal-organic frameworks, nanocubes, carbon nanofibers etc.

- **Based on Pore Dimensions:**

1. Microporous Nano-Materials:

Among all the Nanoporous materials, microporous materials have comparatively small pore sizes. It has a pore diameter of not more than 2nm. Microporous nanomaterials have a very high surface area due to this feature it can show various applications like gas storage, drug delivery, catalysis, and many other applications. Microporous nanomaterials are of three types inorganic framework, organic framework, and hybrid framework (metal-organic framework).

2. Mesoporous Nano-Materials:

Nanoporous compounds that have a pore diameter in the range of 2 to 50 nm are called mesoporous nanomaterials. Mesoporous nanomaterials have larger pore sizes than microporous nanomaterials. Also, it has a high surface area like microporous nanomaterials and it can show applications like microporous nanomaterials. Three important types of mesoporous nanomaterials are mesoporous metal oxides, silica mesoporous materials, and mesoporous carbon.

3. Macroporous Nano-Materials:

In this type of porous nanomaterials, the pore size is greater than 50nm according to IUPAC. These materials can be specified by their large pore size in comparison with micro and mesoporous nanomaterials. They have significant application in the field of tissue engineering, filtration systems etc. Hydrogels are the best example of macroporous nanomaterials, which are used in cell adhesion.

- **Based on Origin:**

1. Natural Nano-Materials:

Nanomaterials produced by nature are specifically called natural nanomaterials. They have a particle size between 1-100 nm. Some examples of naturally occurring nanomaterials are Foraminifera, Spider and silk spider mites, natural colloids etc. Natural nanomaterials are generally used in medicine chemistry, cosmetics, west removal etc.

2. Artificial Nano-Materials:

The nanomaterials produced intentionally at one dimension are called artificially produced nanomaterials. The size of these materials is restricted in the nanoscale. They can reveal unique applications like energy storage, and pharmaceutical industries. Metal-organic framework is one of the examples of artificially produced nanomaterials.

1.3 Synthesis of Nano-Materials:

Materials having at least one dimension in the nanoscale range typically between 1 and 100 nanometers are referred to as nanomaterials. Because of their high surface area to volume ratio and quantum effects, they differ from their bulk counterparts in their physical, chemical, and biological performance. The synthesis of nanomaterials takes place using a couple of main approaches top-down and bottom-up.

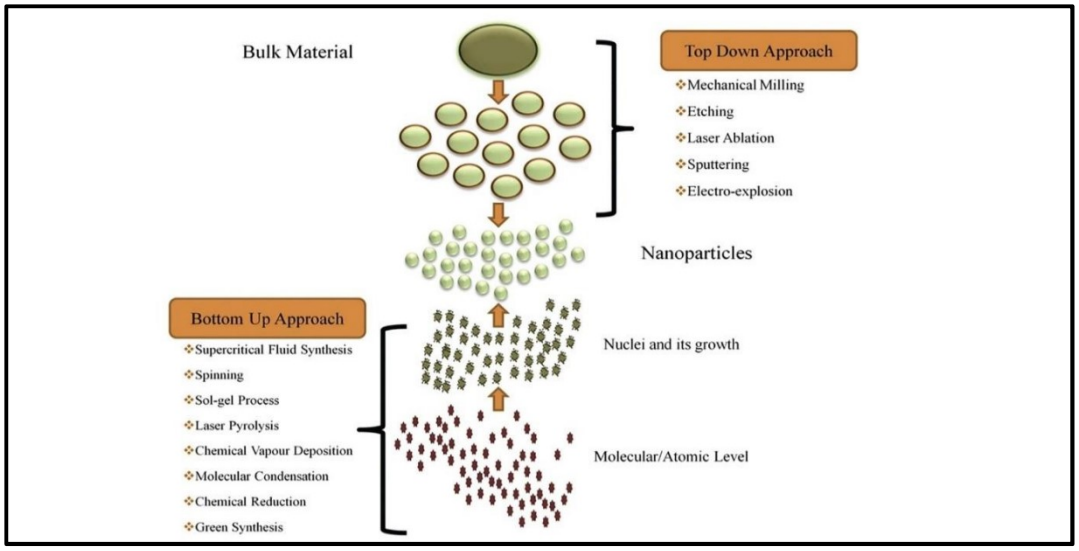

Fig.2 Types of synthesis of Nano-materials

- **Top-Down Approaches:**

Top-down methods involve physically breaking down or dividing larger materials into smaller components. Several examples of this approach include:

1. Mechanical Milling:

Mechanical milling is a commonly used top-down technique for synthesizing nanomaterials. High-energy ball milling facilitates the production of finely dispersed particles within a grain-refined matrix. This method relies on fracture, cold welding, and plastic deformation to modify the particle size, shape, and composition, respectively. Mechanical alloying, which involves grinding elemental or compound powders in an inert atmosphere, enables the formation of amorphous and nanocrystalline alloys as well as metal/non-metal nanocomposites. This technique has been successfully employed to produce a wide range of nanomaterials, including nanoalloys, nanocomposites, and nanocarbons, with high yields. [1]

2. Electrospinning:

Electrospinning is a robust and effective top-down technique for producing continuous nanofibers with diameters ranging from a few nanometers to several hundred nanometers. It is considered one of the most promising methods for large-scale fabrication of nanofibers. During the electrospinning process, a high-voltage electric field is applied to a polymer solution or melt, causing the material to be ejected from the tip of a spinneret and stretched into fine fibers, which are then collected on a grounded surface. [2]

3. Lithography:

Lithography is a top-down approach used in the synthesis of nanomaterials. It involves either the direct patterning of materials using specific radiation or the transfer of a pre-designed geometric pattern known as a mask or master onto a resist-coated semiconductor, typically a silicon wafer.

The lithographic process utilizes three main techniques based on the type of radiation: photolithography, X-ray lithography, and electron beam lithography. The procedure includes several steps such as surface preparation, barrier layer deposition, photoresist application, soft baking, mask alignment, exposure to UV light, development, hard baking, etching, and resist removal. [3]

4. Sputtering:

The sputtering technique involves bombarding solid surfaces with high-energy particles, such as gas ions or plasma, to generate nanomaterials. This method is commonly used to produce nanomaterials without requiring stabilizing agents. Depending on the elemental composition, sputtering can yield nanoparticles typically ranging from 1 to 10 nanometers in diameter. When combined with low-temperature laser ablation, the technique allows for the synthesis of extremely fine materials. Due to its versatility, sputtering is widely utilized in nanomaterial research for producing nanoparticles of various sizes and compositions. [4]

5. The Arc Discharge Method:

The arc discharge method for producing nanomaterials involves vaporizing carbon through the application of an electric field combined with a high-temperature gradient. This process takes place in a vacuum chamber containing two electrodes - a graphite

cathode and an anode. When a high voltage is applied, the anode material sublimates, generating an arc between the electrodes that facilitates the deposition of the material onto a substrate. This technique has been effectively used to synthesize various nanomaterials, including graphene, carbon nanotubes, and silver nanoparticles, which have applications in electronics, energy storage, and biomedicine. [5]

6. Laser Ablation:

By employing laser irradiation to expel material from a surface and generating nonequilibrium vapour conditions, the laser ablation technique is used to create nanomaterials. This method makes use of a powerful laser beam to cause a target material's surface to absorb a substantial quantity of light, which raises the material's temperature quickly and causes it to evaporate into a laser plume. After that, the vaporized material can either condense into particles or clusters not undergoing any chemical reactions, or it can react with reactants added to create fresh substances. [6]

- **Bottom-Up Approaches:**

Bottom-up approach is the method where nano-materials are produced by the simplest construction unit of the materials like atoms, molecules, clusters etc. Common types of bottom-up approaches for the synthesis of nano-materials are:

1. Chemical Vapour Deposition (CVD):

Chemical Vapor Deposition (CVD) is a versatile technique for synthesizing nanomaterials. In this method, vapor-phase precursors are introduced into a hot-wall reactor under conditions that promote nucleation within the vapor phase. CVD allows for the fabrication of a wide range of materials, including doped and multi-component nanoparticles, due to its compatibility with various precursor combinations. By utilizing energy sources such as lasers, plasma, or resistive heating, CVD facilitates chemical reactions among gas molecules to form nanomaterials with controlled size, shape, and properties. This method has been successfully used to produce nanocrystalline materials, binary semiconducting oxide nanobelts, and piezoelectric nanorings, which are applied

in micro- and nano-electromechanical systems as actuators, transducers, and sensors. [7] [8]

2. Solvothermal and Hydrothermal Method:

Nanomaterials can be synthesized using hydrothermal and solvothermal techniques. In hydrothermal synthesis, water serves as the solvent, whereas in the solvothermal method, organic solvents like ethanol, methanol, or acetone are used under high temperature and pressure conditions to produce nanomaterials. Both methods are effective for generating nanomaterials with controlled sizes, shapes, and properties. Compared to hydrothermal synthesis, the solvothermal approach offers advantages such as lower energy consumption and greater environmental sustainability. However, hydrothermal synthesis is more widely studied and commonly applied, as it enables the production of a broad range of nanomaterials, including carbon-based materials, metal oxides, and metal-organic frameworks. [9]

3. Sol-Gel Method:

The sol-gel technique is a very useful method for the synthesis of nanomaterials. Employing alkoxides of metals or solvated metal ingredients, a stable solution (sol) is created. These gels via polycondensation processes to form oxide or alcohol-bridged system. The gel is heat treated to make crystallinity, dried to eliminate volatile elements, and stored to become a solid object. With this process, multiple kinds of oxides, composites, and nanoparticles with specified features can be generated. sol-gel method is a valuable innovation for producing nanomaterials considering its application ranges, low reaction heat, and ease of incorporation of different dopants or activities. [10] [11]

4. Reverse Micelle Methods:

The reverse micelle method is an efficient technique for synthesizing nanostructures. It begins with the formation of water in oil droplets containing the desired reactants. Within these droplets, intermicellar exchange occurs, initiating reactions that lead to the nucleation and growth of nanostructures. Surfactant molecules within the water droplets

dispersed in oil help regulate nanoparticle formation. The final size of the nanoparticles is directly influenced by the droplet size, which in turn depends on factors such as temperature, precursor concentration, the water to surfactant ratio, and the type of surfactant used. This approach offers a straightforward yet powerful means of producing tailored nanomaterials and is applicable to a wide variety of substances. [12]

1.4 Important Features of Nano-Materials:

- **Surface Area:** All nanomaterials have the characteristic of having surface areas that are significantly higher than those of their bulk counterparts. [13]
- **Magnetism:** At the level of the nanosecond, components can exhibit different magnetic behaviours. At the nanoscale, a non-magnetic element may transform into a magnetic. [14]
- **Quantum Effects:** At smaller scales, quantum impacts are more noticeable. The chemical composition of the semiconductor material, however, has an important impact on the dimension at which these effects appear. [15]
- **High Thermal and Electrical Conductivity:** When comparing to their bulk equivalents, exceptional electrical and thermal conductivity can be demonstrated at the nanoscale level based on the characteristics of the nanomaterial. Graphene, which is derived from graphite, is one instance of this. [16]
- **Excellent Mechanical Properties:** Superior mechanical qualities that are lacking in their larger versions are exhibited by nanomaterials. [17]
- **Excellent Support for Catalysts:** The catalyst efficiency has been significantly improved by the excellent dispersion of active catalytic nanoparticles made possible by 2D sheets of different nanomaterials. In an effort to improve performance, catalysts have recently been atomically distributed on 2D nanomaterial sheets. [18]
- **Antimicrobial Activity:** Certain nanomaterials are very effective at treating diseases caused by pathogens because they have antibacterial, antiseptic, and antifungal qualities. [19]

1.5 Application of Nano-Materials:

Nanoparticles composed of elements such as gold, silver, and zinc exhibit unique physicochemical properties that make them highly valuable for medical applications, while platinum is particularly useful in energy storage systems. Silver nanoparticles, in particular, are increasingly being utilized for their optical properties in various products and sensors. Unlike conventional dyes and pigments, silver nanoparticles can efficiently absorb and scatter light, displaying color variations based on their size and shape. Their strong antibacterial properties have led to widespread use in textiles, wound dressings, medical devices, and even household appliances like washing machines and refrigerators. [20] Carbon-based nanomedicines are also widely employed across numerous fields, including drug delivery, enzymatic immobilization, biosensing, medical imaging, and environmental pollutant removal. [21]

- **Catalysis:**

Catalysis was among the earliest applications of nanoparticles, with a wide variety of elements and compounds such as silica, clays, titanium dioxide, iron, and aluminum having long been used as nanoscale catalysts. In recent years, nanocatalysis has gained recognition as a distinct scientific field due to its remarkable activity, selectivity, and efficiency. Metal nanoparticles, especially those in the 1 -10 nm range, often demonstrate superior catalytic performance compared to their bulk counterparts or corresponding metal complexes. This enhanced activity is attributed to several key factors, including a high surface-to-volume ratio, surface geometry effects, electronic interactions, and quantum size effects. Metal nanoparticles dispersed in solution are commonly used as effective heterogeneous catalysts due to their ease of recovery, excellent recyclability, and simplified product separation making them an environmentally friendly option. The catalytic efficiency of nanocatalysts, including conversion rates and selectivity, is strongly influenced by particle size. [22] Catalysts play a crucial role in reducing reaction temperatures, minimizing reagent waste, and enhancing selectivity, thereby helping to prevent undesirable side reactions and contributing to greener chemical processes.

Without catalysts, the production of essential goods such as pharmaceuticals, fine chemicals, polymers, fibers, fuels, paints, and lubricants would not be feasible. [23] In the field of chemistry, carbon nanotubes are widely used in photocatalytic applications

and serve as catalysts in processes like partial oxidation in fuel cells, as well as the synthesis of ammonia and methane. Consequently, catalysts significantly contribute to making industrial processes more cost-effective, sustainable, and environmentally friendly.

- **Water Treatment:**

The use of nanoparticles for the purification of wastewater and water has garnered a lot of interest. Nanomaterials, also have significant specific surface areas and adsorption capabilities because of their small sizes. Different types of nanomaterials have been claimed to be successful in eliminating heavy metals, organic contaminants, inorganic anions, and bacteria. [24] [25] [26] [27] [28] Metal oxide nanoparticles, such TiO_2, have been effectively used in photocatalytic degradation to break down contaminants in water and wastewater in recent years. Due to its non-toxicity, chemical stability, commercial availability, strong photoactivity, etc. TiO_2 has been the subject of extensive research. [29] [30] Contaminants can be oxidized progressively into low molecular weight intermediate compounds in the presence of light and catalyst, and finally, they can change into CO_2, H_2O, and anions like NO^{3-} , PO_4^{3-} , and Cl^-. [31]

- **Sensors:**

The development of a wide variety of nanomaterials has enabled their use in constructing high-performance electrochemical sensing devices for applications in environmental monitoring, food safety, and medical diagnostics. Studies have shown that numerous nanomaterials have been synthesized to detect common chemicals and contaminants often found in food and beverages, including hydrazine (N_2H_4), malachite green (MG), bisphenol A (BPA), ascorbic acid (AA), caffeine, caffeic acid (CA), sulfite (SO_3^{2-}), and nitrite (NO_2^-). Nanotechnology has significantly advanced biosensor technology by enhancing sensitivity and selectivity while also enabling the miniaturization of sensor devices.

In particular, innovative biosensors for glucose monitoring have been developed using fluorescent nanomaterials and nanostructures. These are widely applied in blood glucose meters, which employ electrochemical methods to measure glucose levels [32] [33], an essential tool for individuals with diabetes. Carbon nanotubes have also contributed to the advancement of molecular detection technologies, including gas sensors, small

molecule detectors, electrochemical sensors, and chromatography-based analytical tools. The integration of nanoparticles and other nanomaterials with macroelectrodes improves detection sensitivity and selectivity while also lowering detection limits, making these devices more efficient and accurate. [34]

- **Energy Storage :**

Platinum nanostructures have attracted considerable attention due to their promising applications in energy and environmental catalysis. Thanks to its rich electronic configuration and outstanding catalytic performance, platinum (Pt) plays a vital role in various catalytic processes, including fuel cells, hydrogen generation, organic synthesis, automotive exhaust treatment, and petroleum refining. Platinum-based nanomaterials significantly increase the utilization of Pt atoms by enhancing the number of exposed active sites and expanding the specific surface area. [35] [36]

Researchers at Rice University are exploring carbon nanotube coatings as a means to prevent dendrite formation on lithium-metal anodes, a critical step toward the development of next-generation lithium metal batteries. These batteries have the potential to greatly outperform traditional lithium-ion batteries, offering much faster charging times and nearly ten times higher volumetric energy density. In their work, a multi-walled carbon nanotube layer was applied to lithium metal foil to address stability issues. Additionally, Rice researchers have used carbon nanotubes grown on graphene to develop electrodes with exceptionally high surface area and minimal electrical resistance, which could significantly enhance the performance of energy storage devices.

1.6 Nanomaterials as Photocatalyst :

Because of their special qualities, nanomaterials are becoming more and more recognized for their potential in photocatalytic applications. These substances are appropriate for photocatalytic reactions because of their exceptional photocatalytic activity and broadband gaps in the visible spectrum. In particular, zinc-based, bismuth-based, titanium based semiconductors display these qualities.

Through the nanomaterial's absorption of light, electrons of the valence band are excited to move into the conduction band, which is the mechanism of photocatalysis. Due to

their interaction with the substrate, these electron-hole pairs produce extremely reactive reducing and/or oxidizing radicals on the valence and conduction bands, respectively[37]. [37] Subsequent reactions between these radicals and air or water contaminants lead to their degradation. Numerous variables, including the reaction medium's pH, the kind of photocatalyst, the quantity of the catalyst and contaminant particles, and others, affect how effective photocatalysis is. It has been discovered that nanomaterials are especially useful in heterogeneous photocatalysis - a process that breaks down organic contaminants in air and water by using a catalyst and light. uses of this technique include energy production, biomedical uses, and environmental remediation. [38]

The excellent stability, low cost, great photoactivity, and safety of nanomaterials make them ideal photocatalysts. They may also be made to function in direct sunlight, which makes them a viable tool for environmentally friendly and sustainable applications.

1.7 General Mechanism of Conversion of Organic Species by Photocatalyst:

The ability of nanotechnology, especially semiconducting ones, to work as photocatalysts in the modification of organic molecules in other products has been the focus of much investigation. These nanomaterials, including iron oxide, zinc oxide, and titanium dioxide, have particular characteristics that can allow them to gain light energy effectively and speed up chemical reactions. Photon and the nanomaterial interact during the photocatalytic process, excitation of the material's electrons and the formation of electron-hole pairs. Chemical reactions, such as the breakdown of organic contaminants and the creation of new molecules, are started by these couples. [39] When using a nanomaterial photocatalysts to transform organic substances into another, the following procedures are usually involved:

- **Light Absorption:** When light energy is absorbed in by the nanomaterial, it excites the electrons of substances and generates electron and hole pairs.

- **Electron-Hole Pair Formation:** Two charged particles(i.e. electrons and holes) are created when the excited electrons and holes split apart.
- **Redox Processes**: Redox processes are generated by the electron and hole pairs engaging with the organic species. The contaminants destroyed or changed as a result of these chemical reactions, which display the movement of electrons among the organic species and the nanomaterial.
- **Product Generation:** New developed as a result of redox reactions. These compounds may be the intended products of the photocatalytic reaction or the breakdown products of the original organic molecules. [40]

1.8 Selection of Base Material:

Why Zinc Indium Sulfide?

The well-known catalyst $ZnIn_2S_4$ offers a number of advantages. A number of them are

- **The Visible Light Activity:** $ZnIn_2S_4$ reacts to visible light and has an excellent level of precision resulting in it being helpful in many different domains. $ZnIn_2S_4$ exhibits exceptional photocatalytic activity, especially when it comes to breaking down organic waste. [41]
- **Superior Stability:** The long-term application of $ZnIn_2S_4$ in photocatalytic processes depends on its ability to maintain exceptional thermal and chemical characteristics.
- **Doping Methods:** Doping methods enhance visible light absorption while decreasing the rate of recombination and adjusting the photocatalytic properties of $ZnIn_2S_4$.

- **Nanostructure Engineering:** $ZnIn_2S_4$ photocatalytic activity can be increased and its light-harvesting capacity can be improved by expanding the surface area of nanoparticles.
- **Surface Modes:** $ZnIn_2S_4$ surface modes and band locations must be adjusted in order to optimize photocatalytic activity and raise efficiency. [42]
- **Synthesis Condition Optimization:** $ZnIn_2S_4$ photocatalytic capability can be enhanced by adjusting synthesis parameters including heat, time, and concentration of reactant.
- **Visible Light Responsive for Water Oxidation:** $ZnIn_2S_4$ is a potential material for photo-catalytic water splitting applications since it has been proven to be sensitive to visible light for the oxidation of water. [43]

1.9 Material Selected for Modification:

For better photocatalytic efficiency we need to modify the base material so that a heterostructure is formed between the introduced material and base material and the modified material would give better photocatalytic efficiency.

Why CuS?

- **Excellent Electrical Conductivity:** CuS has good intrinsic conductivity, which facilitates rapid electron transport and reduces charge recombination.This is particularly beneficial when forming heterojunctions (like with ZIS), enhancing charge separation efficiency.
- **Formation of Z-Scheme or Type-II Heterojunctions:** When coupled with ZIS, CuS can participate in a **Z-scheme** or **Type-II** band alignment, depending on the synthesis conditions. This promotes effective charge separation and maintains strong redox potential key for photocatalytic efficiency.
- **Facile Synthesis & Stability:** CuS is easy to synthesize via low-temperature, solution-based methods and is relatively stable in aqueous and photocatalytic environments.

- **High Surface Area (in nanostructured form):** CuS nanostructures (like nanoflakes or nanorods) offer a large surface area, enhancing the number of active sites for photocatalytic reactions.
- **Catalytic Co-catalyst Role:** CuS can also act as a co-catalyst, facilitating charge carrier transfer and improving the photocatalytic hydrogen evolution rate or pollutant degradation.
- **Synergistic Effect in Composites:** In the CuS/ZIS composite, CuS boosts the overall photocatalytic activity by extending light absorption range, promoting charge separation, and enhancing surface reactivity.

1.10 AIM & OBJECTIVE:

Our aim of the experiment is to convert Rhodamine-B(Rh-B) to Rhodamine-110 (Rh-110) under the influence of visible light and photocatalyst.

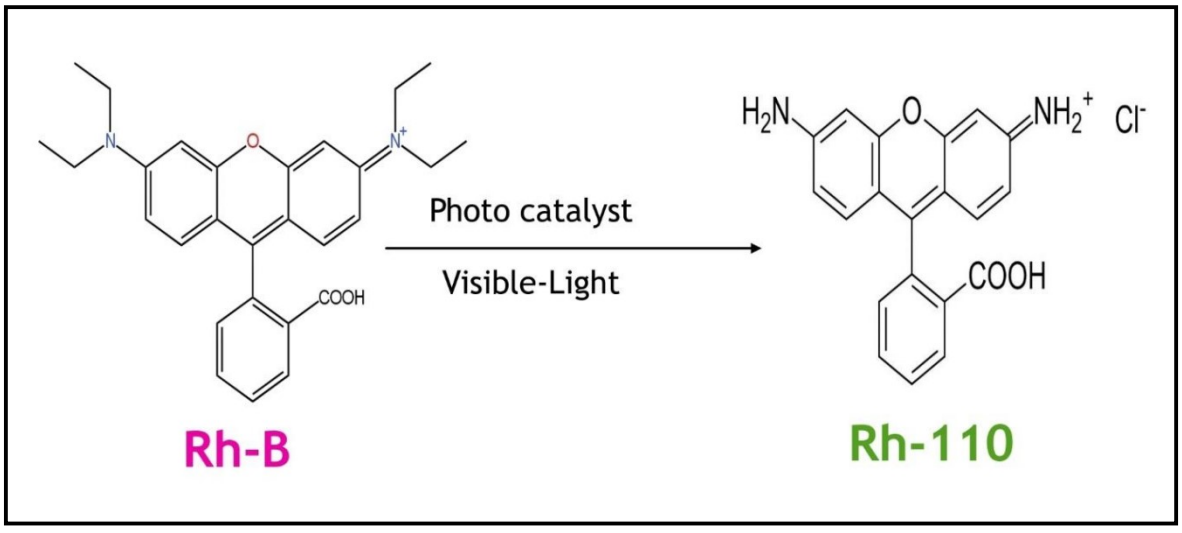

Fig.3 Schematic equation for Rh-B to Rh-110 conversion

- **IMPORTANCE OF Rh-110:**

- **Fluorescence Probe for Proteins:** Rh-110 is a very important tool in microbiology since it acts as a fluorescent active dye to measure the efficiency of enzymes in cells. [44]
- **Serine Protease Substrate:** Serine protease are essential for comprehending enzyme activity and target selectivity, and they are made using Rh- 110.
- **Chemical Immobilization:** Rh-110 is used in chemical immobilization procedures, which highlights its significance in biotechnology. Specifically, it is utilized in the creation of serine protease substrates. [45]
- **Fluorescent Sensors:** Rh-110 is inforced in the creation of fluorescence sensors, demonstrating its abilities in both the analytical and biological realms. These applications include pH testing, anion detection, and bioimaging.
- **Functionalization of Rhodamine Platforms:** To generate a florigenic dye for futuristic optical sensing works, especially in the availability of Fe(III) metal ions, Rh-110 is fabricated with 3-hydroxy-4-pyridinone chelating units. [46]

➢ COMPARISON OF CATALYST ACTIVITY:

Catalyst Used	Time required for conversion	Reference
Bi_3TaO_7-Bi_4TaO_8	480 minutes	[47]
Au-Nanoflower	9 days	[48]
4% CuS/ZIS	90 minutes	Present Work

CHAPTER 2

Experimental Section

2.1 Synthesis of Zinc Indium Sulfide ($ZnIn_2S_4$):

We use the solvothermal (hydrothermal) method for the synthesis.

Requirement:

Zinc Chloride ($ZnCl_2$), Indium Chloride Tetrahydrate ($InCl_3.4H_2O$), Thioacetamide (C_2H_5NS), Distilled water.

Procedure:

The Zinc Indium Sulfide (ZIS) was synthesized using a hydrothermal method. Initially, 60 mL of distilled water was taken in a beaker, followed by the addition of 1 mmol (136.2 mg) of zinc chloride ($ZnCl_2$), 2 mmol (586.4 mg) of indium chloride ($InCl_3.4H_2O$), and 4 mmol (300.5 mg) of thioacetamide (C_2H_5NS). The resulting mixture was stirred for 30 minutes to ensure complete dissolution and uniform mixing of the precursors. After stirring, the solution was transferred to a Teflon-lined stainless steel autoclave and subjected to hydrothermal treatment at 160°C for 12 hours. Upon completion, the autoclave was allowed to cool naturally to room temperature, and the obtained yellow colored precipitate was collected, washed thoroughly with distilled water and ethanol, and dried for further characterization by PXRD technique.

2.2 Synthesis of CuS/ZIS:

We have synthesized four different types of composite by changing the weight percent of copper sulfide precursor. We have synthesized 2%, 4%, 6%, 8% composite respectively.

- **Synthesis of 2%Cus/ZIS:**

Requirement:

Zinc Indium Sulfide, Cuprous Chloride,Sodium Hydroxide, Distilled water.

Procedure:

The 2% CuS/ZIS nanocomposite was prepared using a solution based method at room temperature. Initially, 30 mL of distilled water was added to a beaker containing 100 mg of pre-synthesized Zinc Indium Sulfide (ZIS). The mixture was subjected to ultrasonication for 15 minutes at room temperature to ensure uniform dispersion of ZIS.

Following this, 2.75 mg of copper(I) chloride (CuCl) was introduced into the solution at room temperature, allowing copper ions to interact with the dispersed ZIS. Subsequently, 15 µL of 1 M sodium hydroxide (NaOH) solution was added dropwise under continuous stirring at room temperature. The NaOH served to maintain an alkaline environment, promoting the in-situ formation of CuS nanoparticles on the ZIS surface. Precipitate was collected, washed thoroughly with distilled water and ethanol, and dried for further characterization by PXRD and UV-DRS.

➢ Synthesis of 4%, 6%, 8% Nano-Composites:

The method of preparation is same as the preparation of 2% nanocomposite. Only the amount of precursor taken was different. For 4% composite 5.5 mg of cuprous chloride and 30 µL of 1 M sodium hydroxide were taken. For 6% composite 8.25 mg of cuprous chloride and 45 µL of 1 M sodium hydroxide were taken. For 8% composite 11 mg of cuprous chloride and 60 µL of 1 M sodium hydroxide were taken respectively.

CHAPTER 3

Result and Discussion

3.1 X-Ray Diffraction Analysis:

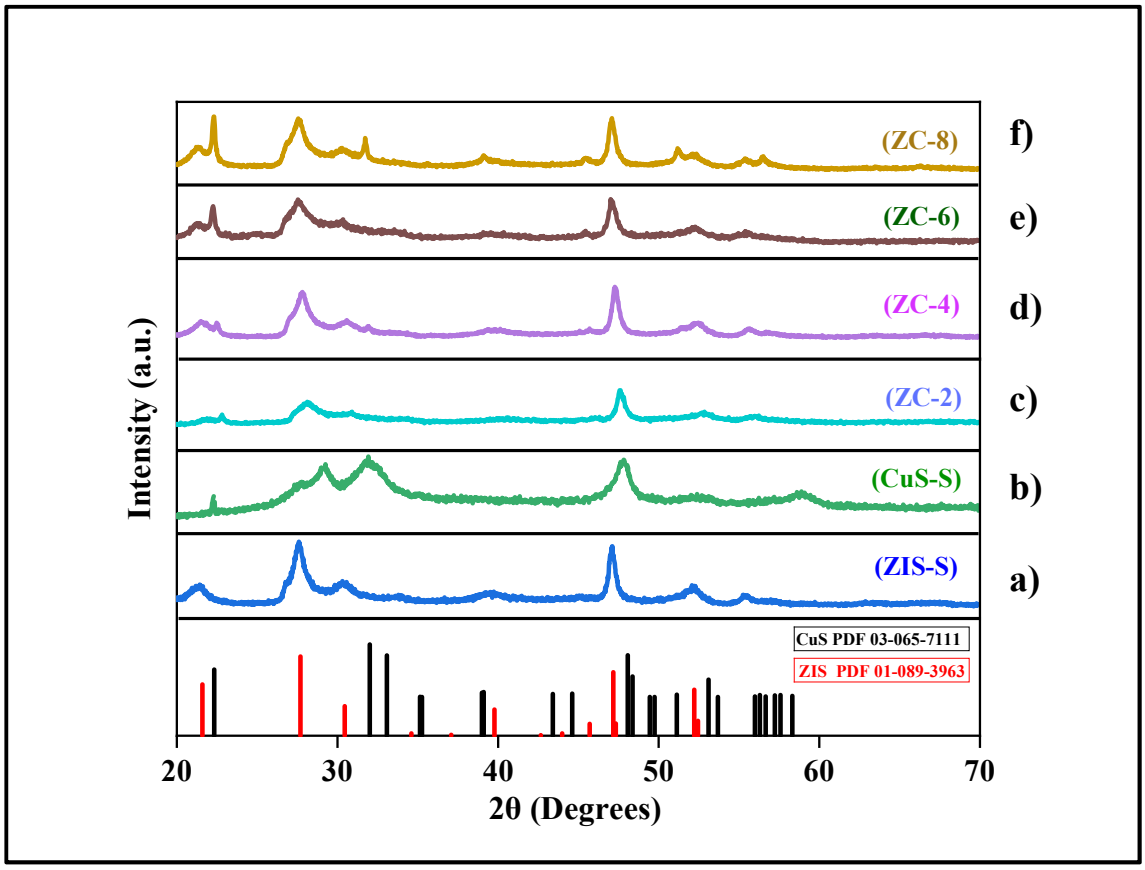

Fig. 4 P-XRD analysis of (a) $ZnIn_2S_4$, (b) CuS, (c) 2% CuS/ZIS, (d) 4% CuS/ZIS, (e) 6% CuS/ZIS, (f) 8% CuS/ZIS

The successful synthesis of Zinc Indium Sulfide (ZIS), Copper Sulfide (CuS), and their nanocomposites (ZC-2, ZC-4, ZC-6, and ZC-8) was confirmed through X-ray diffraction (XRD) analysis. The XRD pattern of the ZIS sample (ZIS-S) displayed distinct diffraction peaks at 2θ values of 22.5°, 47.3°, and 53.4°, which are well matched with the standard JCPDS card no. 01-089-3963 for hexagonal wurtzite ZIS phase, corresponding to the (111), (220), and (311) planes, respectively.

Similarly, the XRD pattern of the CuS sample (CuS-S) exhibited characteristic peaks at 23.2°, 32.7°, 47.9°, and 54.8°, which closely align with the JCPDS card no. 03-065-7111 for hexagonal CuS (covellite phase). These peaks are attributed to the (102), (103), (110), and (108) planes, respectively, validating the successful synthesis of CuS.

In the case of the CuS/ZIS nanocomposites (ZC-2, ZC-4, ZC-6, and ZC-8), the XRD patterns clearly demonstrate the coexistence of both ZIS and CuS. The characteristic peaks of ZIS and CuS were consistently observed across all composite samples, with a noticeable increase in the intensity of CuS peaks with increasing CuS content. Specifically, the peak intensities at 23.2° (CuS (102)) and 32.7° (CuS (103)) became more pronounced in ZC-8, indicating a higher CuS loading. The retention of the main diffraction peaks of ZIS in the composites confirms that the structure of ZIS was preserved during the composite formation.

This XRD analysis confirms the successful synthesis of ZIS and CuS, along with the formation of CuS/ZIS nanocomposites with controlled CuS content.

3.2 UV-DR Spectra:

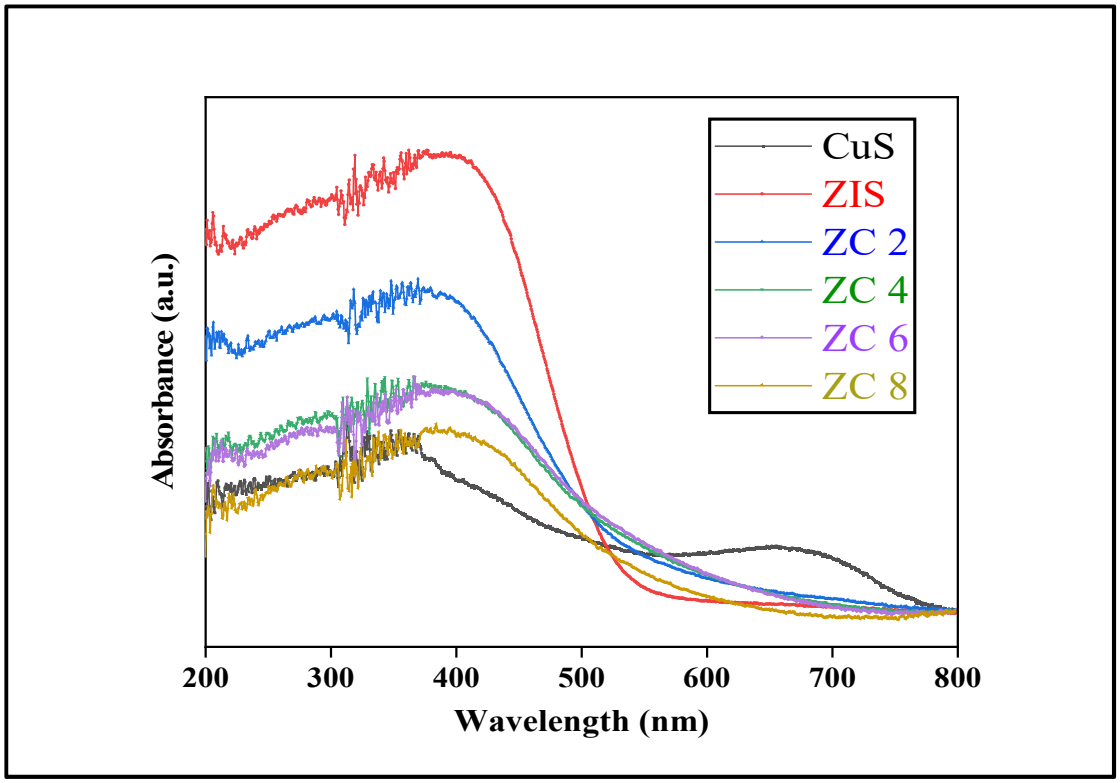

Fig. 5 Normalised DR spectra of (a) $ZnIn_2S_4$, (b) CuS, (c) 2% CuS/ZIS, (d) 4% CuS/ZIS, (e) 6% CuS/ZIS, (f) 8% CuS/ZIS

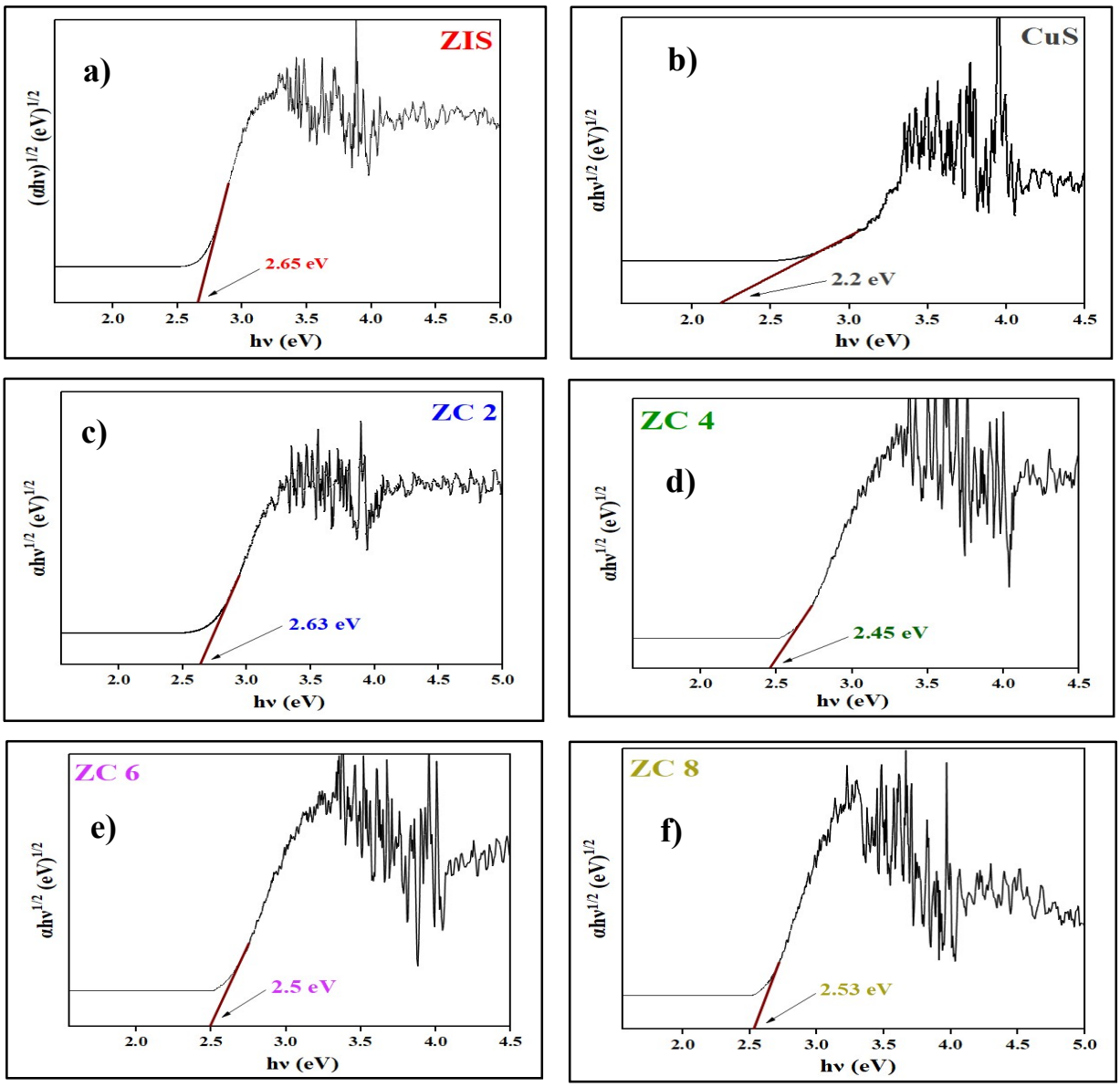

Fig. 6 Tauc plot for band gap calculation of (a) $ZnIn_2S_4$, (b) CuS, (c) 2% CuS/ZIS, (d) 4% CuS/ZIS, (e) 6% CuS/ZIS, (f) 8% CuS/ZIS

The synthesized CuS/ZIS nanocomposites were investigated using UV-Visible diffuse reflectance spectroscopy (UV-DRS), and the results are presented in the form of absorption spectra for pure ZIS, pure CuS, and the CuS/ZIS composites (ZC-2, ZC-4, ZC-6, and ZC-8). The pure ZIS sample exhibited a sharp absorption edge around 470 nm, corresponding to a calculated bandgap of 2.65 eV, which is characteristic of its intrinsic bandgap transition in the visible region. In contrast, pure CuS displayed a broad absorption spectrum extending up to 700 nm, corresponding to a bandgap of 2.2 eV. The calculated bandgap values for the composites were found to be 2.63 eV for ZC-2, 2.45 eV for ZC-4, 2.50 eV for ZC-6, and 2.53 eV for ZC-8, respectively. The slight reduction in bandgap values of the composites compared to pure ZIS indicates strong interfacial interaction between ZIS and CuS, leading to the formation of a CuS/ZIS heterojunction.

CHAPTER 4

Photocatalytic Experiments

Photocatalytic conversion of Rh-B to Rh-110:

A homemade photoreactor with dimensions of 30 cm in height, 25 cm in width, and 25 cm in length was employed for conducting photocatalytic activity experiments. The photoreactor was equipped with a centrally positioned magnetic stirrer to ensure proper mixing during the process. For visible light illumination, two 100 W tungsten filament lamps were used, providing an intensity of approximately 28,000 lux. These lamps were positioned 15 cm above the base of a round-bottom flask to minimize heat generation. Initially photocatalytic reactions were started by taking a different concentration solution of Rhodamine-B (Rh-B) in 100 mL with fixed amount (10 mg) of 4% CuS/ZIS catalyst to complete the optimisation of concentration followed by optimisation of catalytic dose, keeping concentration constant. The conversion of Rh-B to Rh-110 was initiated by turning on the lamps. At every 30 minutes, a 3 ml aliquot was withdrawn and subjected to centrifugation to separate the photocatalyst, then the sample was investigated in a UV-visible spectrophotometer to check the rate of conversion. It was also observed that alone ZIS (base material) and CuS (loading material) were unable to show the conversion, only nano-composites were showing the conversion.

4.1 Concentration Optimisation of Rh-B:

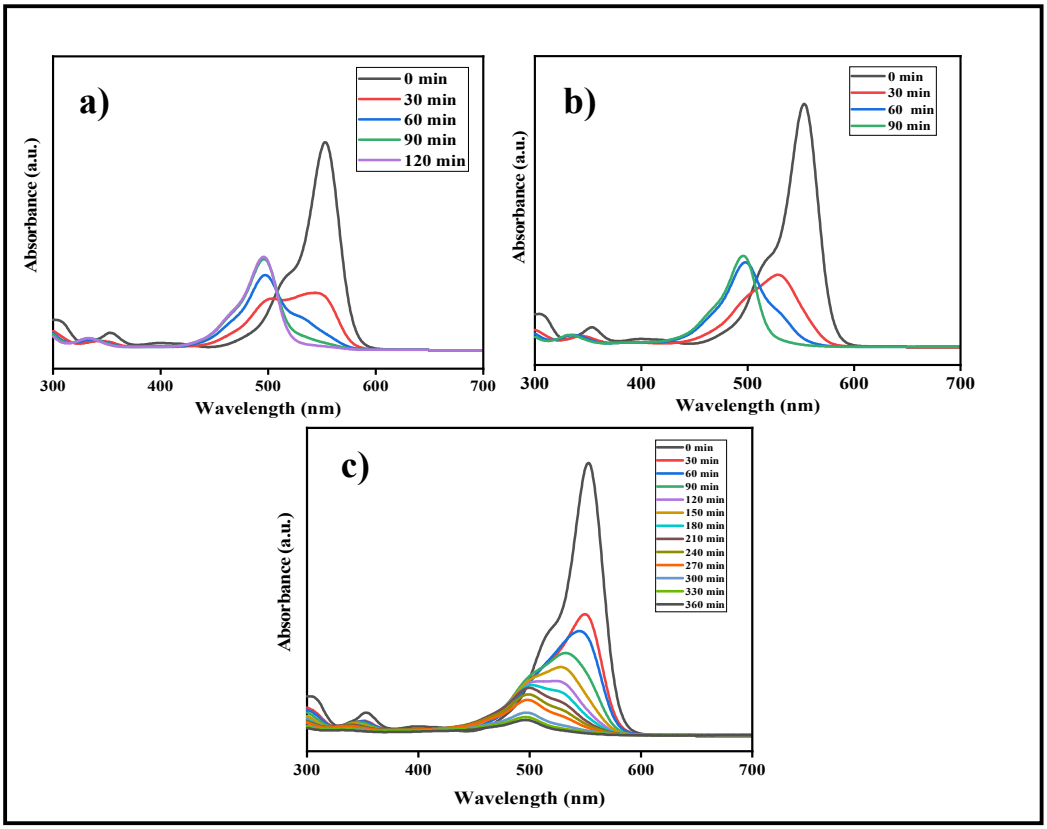

Fig. 7 UV-Vis Spectra of the conversion of (a) 5 ppm Rh-B to Rh-110 using 10 mg 4% CuS/ZIS, (b) 7.5 ppm Rh-B to Rh-110 using 10 mg 4% CuS/ZIS, (c) 10 ppm Rh-B to Rh-110 using 10 mg 4% CuS/ZIS

The catalytic conversion of Rh-B to Rh-110 was systematically studied at different initial concentrations of Rh-B (5 ppm, 7.5 ppm, and 10 ppm) using a constant catalyst dose of 10 mg. The UV-Visible spectra of the reaction mixtures recorded at regular time intervals clearly demonstrate a progressive decrease in the characteristic absorption peak of Rh-B at 554 nm, along with the simultaneous emergence of a new peak at 496 nm, corresponding to Rh-110. This observable shift in wavelength from 554 nm to 496 nm confirms the successful conversion of Rh-B to Rh-110.

Among the tested concentrations, the 7.5 ppm solution of Rh-B demonstrated the most efficient conversion, achieving complete transformation within 90 minutes. The 10 ppm solution, on the other hand, required a significantly longer duration of 360 minutes for complete conversion with degradation. The 5 ppm solution took 120 minutes for the

conversion. We selected 7.5 ppm as the optimized concentration since it offers a higher reactant availability and less time for the conversion.

4.2 Dose Optimisation:

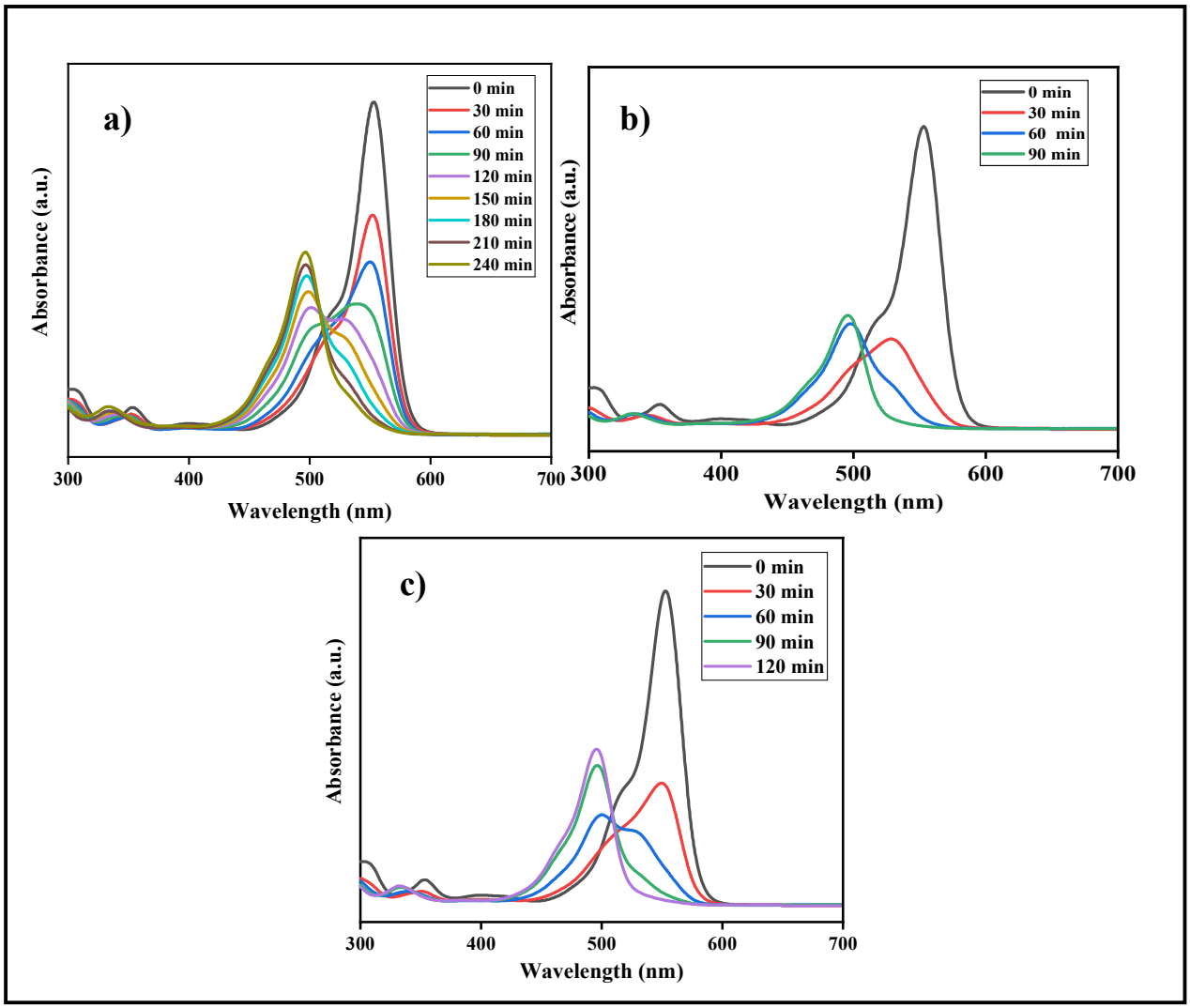

Fig. 8 UV-Vis Spectra of conversion of 7.5 ppm Rh-B to Rh-110 using (a) 5 mg 4% CuS/ZIS, (b) 10 mg 4% CuS/ZIS, (c) 15 mg 4% CuS/ZIS

The optimization of the catalytic dose for the conversion of Rh-B to Rh-110 was systematically investigated using 5 mg, 10 mg, and 15 mg of the catalyst while maintaining a constant Rh-B concentration of 7.5 ppm. At 5 mg of catalyst, complete conversion of Rh-B to Rh-110 required 240 minutes, as indicated by the gradual decrease of the Rh-B peak at 554 nm and the corresponding increase at 496 nm, characteristic of Rh-110. When the catalyst amount was increased to 10 mg, the conversion time

significantly reduced to 90 minutes, maintaining the characteristic spectral shift. In contrast, further increasing the catalyst dose to 15 mg, conversion was achieved in 120 minutes. These observations confirm that increasing the catalyst amount beyond 10 mg does not further enhance the reaction rate.

After both the optimisations, the best fitted condition for efficient conversion of Rh-B to Rh-110 was determined to be 7.5 ppm Rh-B with 10 mg catalyst, achieving a balance between reaction time and catalyst efficiency using 4% CuS/ZIS nano-composite.

4.3 Comparison of Optimised Condition on composites:

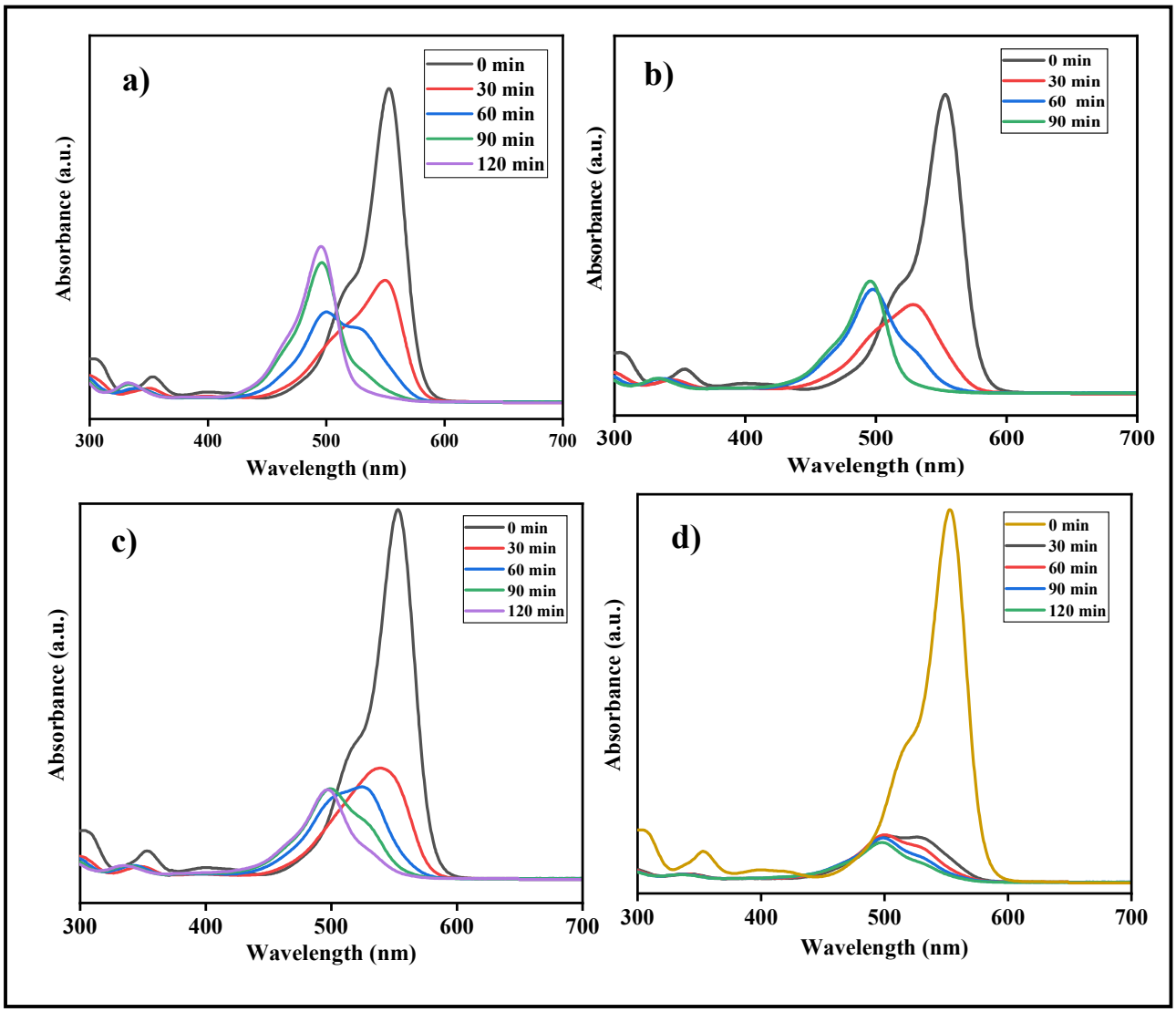

Fig. 9 UV-Vis Spectra of conversion of 7.5 ppm Rh-B to Rh-110 using 10 mg (a) 2% CuS/ZIS, (b) 4% CuS/ZIS, (c) 6% CuS/ZIS, (d) 8% CuS/ZIS

The optimised condition was applied on all the four composites, and it was found that 2% CuS/ZIS took 120 minutes for the complete conversion whereas 4% composite showed the conversion within 90 minutes only. It was observed that 6% and 8% composite did not show complete conversion in 120 minutes, and 8% composite showed higher rate of degradation. It was confirmed with the performed analysis that 4% composite was most efficient for the conversion of Rh-B to Rh-110.

4.4 Plausible Mechanism for the Photocatalytic Transformation of Rh-B to Rh-110:

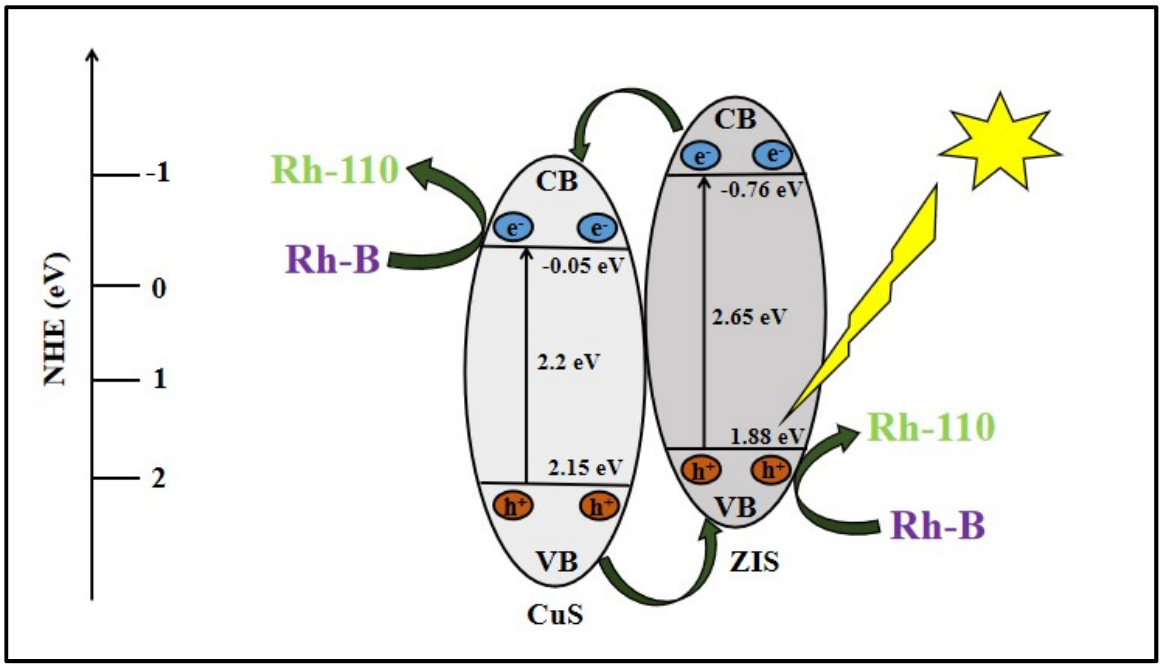

Fig. 10 Plausible Mechanism for The Conversion of Rh-B to Rh-110

The plausible mechanism for the conversion of Rh-B to Rh-110 using the CuS/ZIS heterostructure under visible light illumination involves a stepwise deethylation process. Initially, upon irradiation with visible light, the CuS/ZIS heterostructure is excited, generating electron-hole pairs. The photogenerated electrons in the conduction band (CB) of ZIS migrate to the CB of CuS due to the favorable band alignment, while the holes remain in the valence band (VB) of ZIS. This efficient charge separation minimizes electron-hole recombination, significantly enhancing the photocatalytic activity.

The excited electrons on CuS participate in the reduction of Rh-B, leading to the formation of an excited radical cation ($Rh\text{-}B^{\bullet+}$). This radical undergoes a series of deethylation reactions. In the first step, a single ethyl group is removed, forming a partially deethylated product. Successive excitation and electron transfer continue the deethylation process, ultimately converting Rh-B to Rh-110. The deethylation is facilitated by the active sites on the catalyst surface and the photogenerated electrons, which attack the carbon-nitrogen bonds of the ethyl groups, leading to their cleavage.

The migration of electrons from ZIS to CuS ensures that CuS remains electron-rich, promoting the reduction steps required for this transformation. The final product, Rh-110, is confirmed by the characteristic absorption shift from 554 nm (Rh-B) to 496 nm (Rh-110), as evidenced by the UV-Vis spectra. [49] [50]

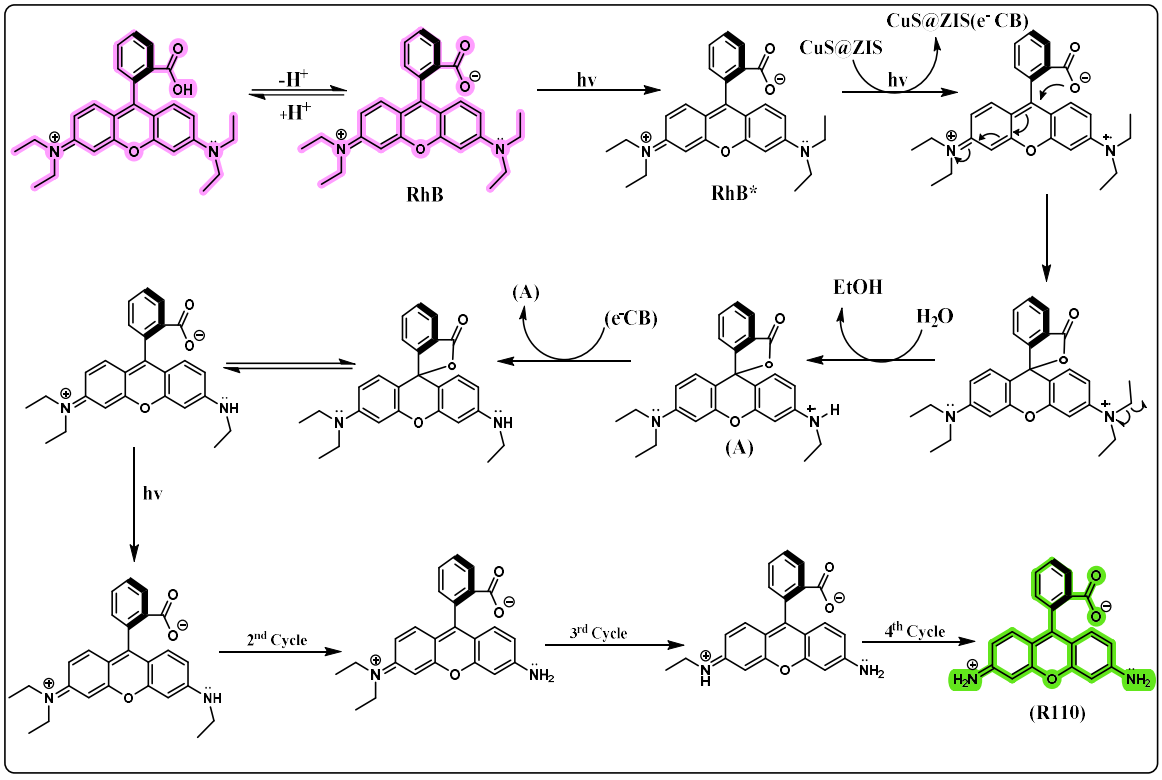

Fig. 11 Stepwise deethylation of Rh-B

4.5 Evidence of Rh-110 Production by Spectral Analysis :

The UV-Vis absorption spectrum of standard Rh-110 (ST Rh-110) displayed an absorption peak at 496.5 nm. Remarkably, the absorption peak of the converted product (Rh-110) perfectly matched this value, providing strong initial evidence for its formation as shown in fig. 13(a). To further substantiate this observation, steady-state fluorescence emission measurements were conducted. The converted product exhibited an emission peak precisely at 520 nm, which was in excellent agreement with the standard Rh-110, reinforcing the successful conversion (fig.13(b)). For additional confirmation, the excitation spectra corresponding to the emission at 520 nm were also recorded. This

spectra revealed an excitation peak at exactly 496.5 nm, confirming the emission at 520 nm as shown in fig. 13(c).

The consistent alignment of the absorption, emission, and excitation spectra between the ST Rh-110 and the Rh-110 unequivocally confirms the successful formation of Rhodamine 110.

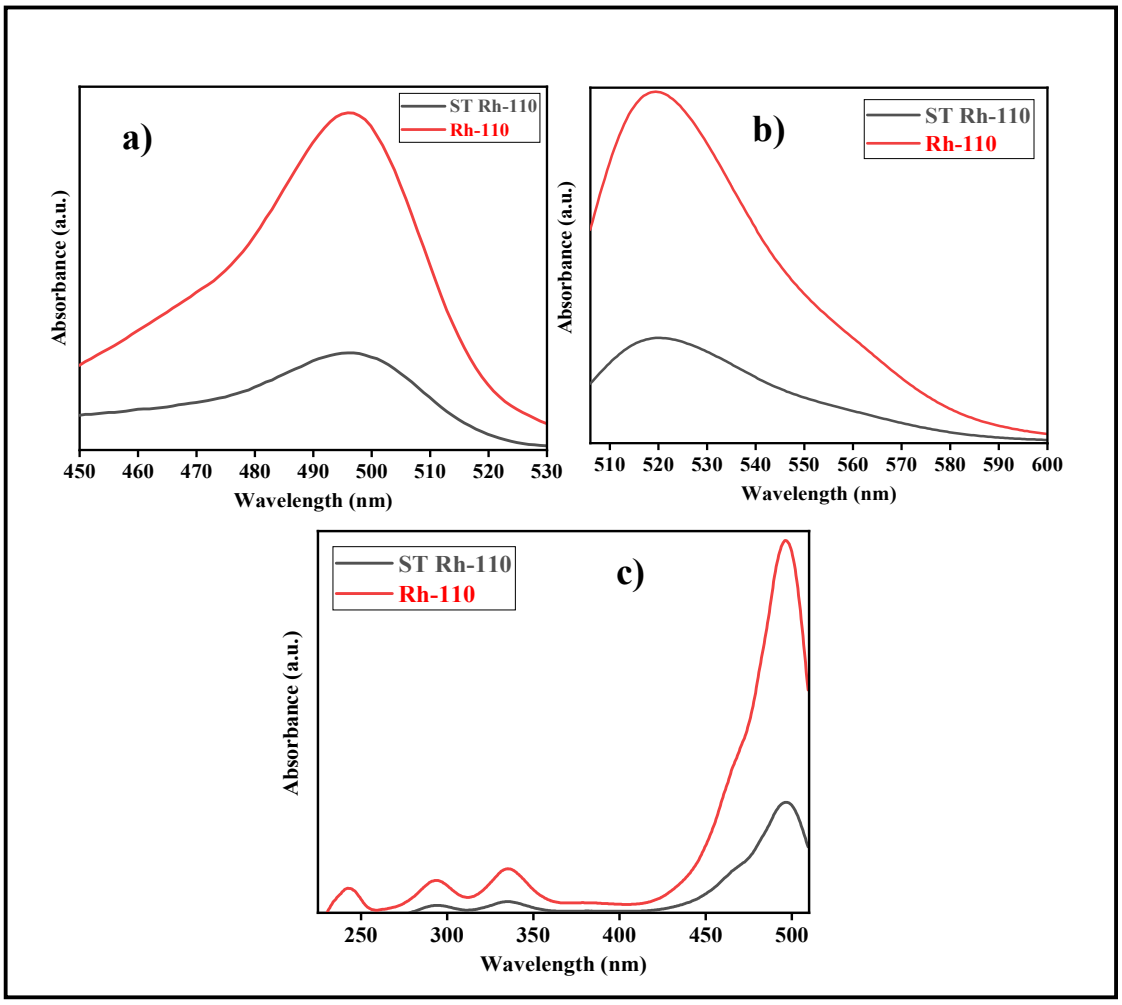

Fig. 12 (a) Absorption Spectra, (b) Emission Spectra, (c) Excitation Spectra of Standard Rh-110 (ST Rh-110) and photocatalytic product (Rh-110)

CHAPTER 5

Conclusion

5.1 Conclusion

The successful formation of CuS/ZIS heterostructures was confirmed, and their photocatalytic performance was systematically evaluated for the conversion of Rh-B to Rh-110. Among the various composites (2%, 4%, 6%, and 8% CuS/ZIS), the 4% CuS/ZIS demonstrated the highest photocatalytic efficiency. This optimized performance can be directly attributed to its ideal band gap of 2.45 eV, which offers a perfect balance between light absorption and charge separation. The band gap of 4% CuS/ZIS is significantly lower than that of pure ZIS (2.65 eV), enabling better light absorption, yet it maintains an efficient electron-hole separation due to the heterojunction formation.

Interestingly, despite CuS having an even lower band gap of 2.2 eV, it showed poor photocatalytic activity when used alone. This is due to the rapid recombination of photogenerated electron-hole pairs in pure CuS, a common problem in narrow-bandgap semiconductors.

The optimized condition for the conversion of Rh-B to Rh-110 was determined to be 7.5 ppm Rh-B with a catalyst dose of 10 mg, achieving complete conversion within 90 minutes by 4% CuS/ZIS nano-composite.

The study demonstrates that the successful formation of a Type II heterostructure between CuS and ZIS not only improves the light absorption range of ZIS but also enables efficient charge separation, which is critical for enhancing photocatalytic performance. The carefully optimized reaction conditions and the strategic use of a 4% CuS loading establish this composite as an efficient and practical photocatalyst for the conversion of Rh-B to Rh-110. This work provides a valuable understanding of heterostructure design and its impact on photocatalytic activity, paving the way for further advancements in photocatalyst development for environmental and energy applications.

References

[1] T. Prasad Yadav, R. Manohar Yadav and D. Pratap Singh, Nanosci. Nanotechnol., 2012, 2, 22–48.

[2] R. Ostermann, J. Cravillon, C. Weidmann, M. Wiebcke and B. M. Smarsly, Chem. Commun., 2011, 47, 442-444.

[3] Colson, Pierre, Catherine Henrist, and Rudi Cloots. "Nanosphere lithography: a powerful method for the controlled manufacturing of nanomaterials." Journal of Nanomaterials 2013 (2013): 21-21.

[4] Liang, Jie, Qian Liu, Tingshuai Li, Yonglan Luo, Siyu Lu, Xifeng Shi, Fang Zhang, Abdullah M. Asiri, and Xuping Sun. "Magnetron sputtering enabled sustainable synthesis of nanomaterials for energy electrocatalysis." Green Chemistry 23, no. 8 (2021): 2834-2867.

[5] Su, Y. and Zhang, Y., 2015. Carbon nanomaterials synthesized by arc discharge hot plasma. Carbon, 83, pp.90-99.

[6] Kim, Myungjoon, Saho Osone, Taesung Kim, Hidenori Higashi, and Takafumi Seto. "Synthesis of nanoparticles by laser ablation: A review." KONA Powder and Particle Journal 34 (2017): 80-90.

[7] Manawi, Yehia M., Ihsanullah, Ayman Samara, Tareq Al-Ansari, and Muataz A. Atieh. "A review of carbon nanomaterials' synthesis via the chemical vapor deposition (CVD) method." Materials 11, no. 5 (2018): 822.

[8] Dillon, A. C., A. H. Mahan, Rohit Deshpande, J. L. Alleman, J. L. Blackburn, P. A. Parillia, M. J. Heben et al. "Hot-wire chemical vapor synthesis for a variety of nano-materials with novel applications." Thin Solid Films 501, no. 1-2 (2006): 216-220.

[9] Li, Jianlin, Qingliu Wu, and Ji Wu. "Synthesis of Nanoparticles via Solvothermal and Hydrothermal Methods 12." (2016)

[10] 10 Bokov, Dmitry, Abduladheem Turki Jalil, Supat Chupradit, Wanich Suksatan, Mohammad Javed Ansari, Iman H. Shewael, Gabdrakhman H. Valiev, and Ehsan Kianfar. "Nanomaterial by sol-gel method: synthesis and application." Advances in Materials Science and Engineering 2021 (2021): 1-21.

[11] Hayle, Stotaw Talbachew, and Girma Goro Gonfa. "Synthesis and characterization of titanium oxide nanomaterials using sol-gel method." American Journal of Nanoscience and Nanotechnology 2, no. 1 (2014): 1.

[12] Eastoe, Julian, Martin J. Hollamby, and Laura Hudson. "Recent advances in nanoparticle synthesis with reversed micelles." Advances in colloid and interface

science 128 (2006): 5-15.

[13] Eastoe, Julian, Martin J. Hollamby, and Laura Hudson. "Recent advances in nanoparticle synthesis with reversed micelles." Advances in colloid and interface science 128 (2006): 5-15.

[14] Roduner, Emil. "Size matters: why nanomaterials are different." Chemical society reviews 35, no. 7 (2006): 583-Rodu.

[15] Geoffrion, Luke D., and Grégory Guisbiers. "Quantum confinement: size on the grill!." Journal of Physics and Chemistry of Solids 140 (2020): 109320.

[16] Krishnan, Siva Kumar, Eric Singh, Pragya Singh, Meyya Meyyappan, and Hari Singh Nalwa. "A review on graphene-based nanocomposites for electrochemical and fluorescent biosensors." RSC advances 9, no. 16 (2019Nanotechnolog.

[17] Wu, Qiong, Wei-shou Miao, Yi-du Zhang, Han-jun Gao, and David Hui. "Mechanical properties of nanomaterials: A review." Nanotechnology Reviews 9, no. 1 (2020): 259-273.

[18] Liu, Xin, Meng Xu, Lingyun Wan, Hongdan Zhu, Kexin Yao, Roberto Linguerri, Gilberte Chambaud, Yu Han, and Changgong Meng. "Superior catalytic performance of atomically dispersed palladium on graphene in CO oxidation." ACS Catalysis 10, no. 5 (2020): 3084-3093.

[19] Castro, Edison, Andrea Hernandez Garcia, Gerardo Zavala, and Luis Echegoyen. "Fullerenes in biology and medicine." Journal of Materials Chemistry B 5, no. 32 (2017): 6523-6535.

[20] Rineesh, N. R., M. S. Neelakandan, and S. J. J. N. N. Thomas. "Applications of silver nanoparticles for medicinal purpose." JSM Nanotechnol Nanomed 6, no. 1 (2018): 1063.

[21] Chen, Ming, Xiaosheng Qin, and Guangming Zeng. "Biodegradation of carbon nanotubes, graphene, and their derivatives." Trends in biotechnology 35, no. 9 (2017): 836-846.

[22] Li, Gao, and Rongchao Jin. "Catalysis by gold nanoparticles: carbon-carbon coupling reactions." Nanotechnology Reviews 2, no. 5 (2013): 529-545.

[23] Singh, Santosh Bahadur, and Praveen Kumar Tandon. "Catalysis: a brief review on nano-catalyst." J Energy Chem Eng 2, no. 3 (2014): 106-115.

[24] W.-W. Tang, G.-M. Zeng, J.-L. Gong et al., ―Impact of humic/fulvic acid on the removal of heavy metals fromaqueous solutions using nanomaterials: a review,‖ Science of the Total Environment, vol. 468-469, pp. 1014–1027, 2014.

[25] Yan J., L. Han,W. Gao, S. Xue, andM.Chen, ―Biochar supported nanoscale

zerovalent iron composite used as persulfate activator for removing trichloroethylene,‖ Bioresource Technology, vol. 175, pp. 269–274, 2015.

[26] Liu F., Yang J. H., Zuo J. et al., ―Graphene-supported nanoscale zero-valent iron: removal of phosphorus from aqueous solution and mechanistic study,‖ Journal of Environmental Sciences, vol. 26, no. 8, pp. 1751– 1762, 2014.

[27] Kalhapure R. S., Sonawane S. J., Sikwal D. R. et al., ―Solid lipid nanoparticles of clotrimazole silver complex: an efficient nano antibacterial against Staphylococcus aureus and MRSA, Colloids and Surfaces B: Biointerfaces, vol. 136, pp. 651–658, 2015.

[28] Haijiao Lu, Jingkang Wang, Marco Stoller, Ting Wang, Ying Bao, Hongxun Hao, An Overview of Nanomaterials for Water and Wastewater Treatment, Advances in Materials Science and Engineering, Volume 2016, Article ID 4964828, http://dx.doi.org/10.1155/2016/496.

[29] Zhao, Z.M.; Sun, J.; Xing, S.M.; Liu, D.J.; Zhang, G.J.; Bai, L.J.; Jiang, B.L. Enhanced Raman scattering and photocatalytic activity of TiO2 films with embedded Ag nanoparticles deposited by magnetron sputtering. J. Alloys Compd. 2016, 679, 88–93.

[30] Guo, Q.; Zhou, C.Y.; Ma, Z.B.; Ren, Z.F.; Fan, H.J.; Yang, X.M. Elementary photocatalytic chemistry on TiO2 surfaces. Chem. Soc. Rev. 2016, 45, 3701–3730.

[31] A. Bratovcic, Photocatalytic degradation of organic compounds in wastewaters, Technologica acta, ISSN 18400426, accepted review paper, 2019.

[32] Venkatesh S. Manikandan, BalRam Adhikari, Aicheng Chen, Nanomaterial based electrochemical sensors for the safety and quality control of food and beverages, Analyst, 19, 2018.

[33] Longyi Chen, Eugene Hwang, Jin Zhang, Fluorescent Nanobiosensors for Sensing Glucose, Sensors 2018, 18(5), 1440; doi:10.3390/s18051440.

[34] Brainina Kh., Stozhko N., Bukharinova M., Vikulova E., Nanomaterials: Electrochemical Properties and Application in Sensors, Physical Sciences Reviews, Vol. 3, 9, 2018, doi: https://doi.org/10.1515/psr-2018-8050.

[35] Sibin Duan, Zhe Du, Hongsheng Fan, Rongming Wang, Nanostructure Optimization of Platinum-Based Nanomaterials for Catalytic Applications, nanomaterials, 2018, 8, 949; doi:10.3390/nano8110949.

[36] Wolf, O.; Dasog, M.; Yang, Z.; Balberg, I.; Veinot, J.G.; Millo, O. Doping and quantum confinement effects in single Si nanocrystals observed by scanning tunneling spectroscopy. Nano Lett. 2013, 13, 2516–2521.

[37] Feliczak-Guzik, Agnieszka. "Nanomaterials as photocatalysts—synthesis and their

potential applications." Materials 16, no. 1 (2022): 193.

[38] Krishna, Prashanth Gopala, Prabhu Chandra Mishra, Mutthuraju Mahadev Naika, Manoj Gadewar, Prashanth Paduvarahalli Ananthaswamy, Srilatha Rao, Sivadhas Rosejanet Boselin Prabhu et al. "Photocatalytic activity induced by metal nanoparticles synthesized by sustainable approaches: a comprehensive review." Frontiers in Chemistry 10 (2022): 917831.

[39] Jaiswal, Komal, Madhusmita Mahanta, and Mrinmoy De. "Nanomaterials in photocatalysed organic transformations: development, prospects and challenges." Chemical Communications (2023).

[40] Rosso, Cristian, Giacomo Filippini, Alejandro Criado, Michele Melchionna, Paolo Fornasiero, and Maurizio Prato. "Metal-free photocatalysis: two-dimensional nanomaterial connection toward advanced organic synthesis." ACS nano 15, no. 3 (2021): 3621-3630.

[41] Elaouni, Aicha, M. El Ouardi, A. BaQais, Madjid Arab, M. Saadi, and H. Ait Ahsaine. "Bismuth tungstate Bi 2 WO 6: a review on structural, photophysical and photocatalytic properties." RSC advances 13, no. 26 (2023): 17476-17494.

[42] Zhang, Liwu, and Yongfa Zhu. "A review of controllable synthesis and enhancement of performances of bismuth tungstate visible-light-driven photocatalysts." Catalysis Science & Technology 2, no. 4 (2012): 694-706.

[43] Trixy Nimmy Priscilla, D., R. Radha, A. Chitra, and S. K. Geetha. "Comprehensive Evaluation of Nanosized Bismuth Tungstate (Bi_2WO_6) as Photoanodes for Photoelectrochemical Water Splitting Performance." Journal of Cluster Science 35, no. 3 (2024): 875-889.

[44] Das, Ranjita S., Swapnil K. Warkhade, Anupama Kumar, G. S. Gaikwad, and Atul V. Wankhade. "Graphitic carbon nitride@ silver zirconate nanocomposite (gC_3N_4@ Ag_2ZrO_3): a Type-II heterojunction for an effective visible light photocatalysis and bacterial photo-inactivation." Journal of Alloys and Compounds 846 (2020):

155770.

[45] Beija, Mariana, Carlos AM Afonso, and José MG Martinho. "Synthesis and applications of Rhodamine derivatives as fluorescent probes." Chemical Society Reviews 38, no. 8 (2009): 2410-2433.

[46] Queirós, Carla, Sílvia Vinhas, Jéssica Oliveira, Andreia Leite, Ana MG Silva, and Maria Rangel. "Functionalization of Rhodamine Platforms with 3-Hydroxy-4-pyridinone Chelating Units and Its Fluorescence Behavior towards Fe (III)." Molecules 27, no. 5 (2022): 1567.

[47] Banoo, Maqsuma, Kaustav Chatterjee, Sanjit Mondal, C. P. Vinod, and Ujjal K. Gautam. "A ‘self- activating’Bi 3 TaO 7–Bi 4 TaO 8 Br photocatalyst and its use in the sustainable production of pro-fluorophoric rhodamine-110." Green Chemistry 24, no. 14 (2022): 5514-5523.

[48] “Bera, Kallol, Tanmay Ghosh, and Soumen Basak. "Synthesis of chiral, crystalline Au-nanoflower catalyst assisting conversion of rhodamine-B to rhodamine-110 and a single-step, one-pot, eco-friendly reduction of nitroarenes." The Journal of Physical Chemistry C 119, no. 4 (2015): 1800-1808.

[49] Khanam, Shomaila, and Sanjeeb Kumar Rout. "Enhanced photocatalytic oxidation of RhB and MB using plasmonic performance of Ag deposited on Bi_2WO_6." Chemistry 4, no. 2 (2022): 272-296.

[50] Banoo, Maqsuma, Kaustav Chatterjee, Sanjit Mondal, C. P. Vinod, and Ujjal K. Gautam. "A ‘self- activating’Bi 3 TaO 7–Bi 4 TaO 8 Br photocatalyst and its use in the sustainable production of pro-fluorophoric rhodamine-110." Green Chemistry 24, no. 14 (2022): 5514-5523.